Biomedical Ti–Mo Alloys with Surface Machined and Modified by Laser Beam: Biomechanical, Histological, and Histometric Analysis in Rabbits

Nilson T.C. Oliveira, PhD;*† Fernando P.S. Guastaldi, MSc;* Vittoria Perrotti, DDS, PhD;† Eduardo Hochuli-Vieira, MD, DDS;‡ Antonio C. Guastaldi, PhD;* Adriano Piattelli, MD, DDS;† Giovanna Iezzi, DDS, PhD†

ABSTRACT

Purpose: *In vivo* bone response was assessed by removal torque, hystological and histometrical analysis on a recently developed biomedical Ti-15Mo alloy, after surface modification by laser beam irradiation, installed in the tibia of rabbits.

Materials and Methods: A total of 32 wide cylindrical Ti-15Mo dental implants were obtained (10 mm × 3.75 mm). The implants were divided into two groups: 1) control samples (Machined surface – MS) and 2) implants with their surface modified by Laser beam-irradiation (Test samples – LS). Six implants of each surface were used for removal torque test and 10 of each surface for histological and histometrical analysis. The implants were placed in the tibial metaphyses of rabbits.

Results: Average removal torque was 51.5 Ncm to MS and >90 Ncm to LS. Bone-to-implant-contact percentage was significantly higher for LS implants both in the cortical and marrow regions.

Conclusions: The present study demonstrated that laser treated Ti-15Mo alloys are promising materials for biomedical application.

KEY WORDS: bone histomorphometry, laser beam surface modification, removal torque, Ti–Mo alloys, titanium alloys, wettability

INTRODUCTION

The population of most countries is increasing so the necessity to substitute hard tissue devices such as bone and teeth is growing, and then the demand for dental and orthopedic implants has been growing, thus requiring more investigations on metals and alloys for this goal.[1–3] Titanium (Ti) and its alloys have been extensively used in the last decades for medical devices and orthopedic and dental implants because of their superior qualities, such as high corrosion resistance, appropriate mechanical properties, low elasticity modulus, and good local and systemic biocompatibility.[1–5]

In general, Ti alloys exceed the mechanical properties of pure Ti for orthopedic applications.[4] For example, Ti–6Al–4V alloy has become one of the most used biomaterials in orthopedic applications because of its high corrosion resistance and good mechanical properties.[2,4,6–9] However, when the Ti–6Al–4V alloy is implanted into a physiological in vivo environment, its electrochemical stability is affected, resulting in increased metal ion release.[10] Indeed, the main cause of Ti–6Al–4V concerns are the cytotoxicity of Vanadium (V) and the possible occurrence of Alzheimer's disease related to the presence of Aluminum (Al) ions;[2,4,6–9] this lead to the necessity of replacement of these alloys for medical applications such as orthopedic implants.[7]

Therefore, growing interest has been recently observed in the development of materials prepared with nontoxic elements such as Nb, Ta, Zr, and Mo.[2,4] Attempts were made to develop Ti alloys of different

*Biomaterials Group, IQ, Universidade Estadual Paulista, UNESP, Araraquara, SP, Brazil; †Department of Stomatology, Dental School, University of Chieti-Pescara, Chieti, Italy; ‡Departamento de Diagnóstico e Cirurgia, Faculdade de Odontologia de Araraquara, Universidade Estadual Paulista, UNESP, Araraquara, SP, Brazil

Reprint requests: Dr. Nilson T.C. Oliveira Ph.D., Biomaterials Group, IQ, Universidade Estadual Paulista – UNESP. Rua Francisco Degni, S/N, CEP. 14.901-800, Araraquara, SP, Brazil; e-mail: ntco@yahoo.com

DOI 10.1111/j.1708-8208.2011.00354.x

compositions to achieve better performance in terms with biomechanical compatibility (by reducing the Young's modulus) and biochemical compatibility (by excluding toxic elements).[5] The stiffness of a metal is determined by its Young's modulus as well as its area of moment inertia. In the case of dental implants, the Young's modulus is far higher than that of the cortical bone: that of pure Ti is 112 GPa, Ti–6Al–4V alloy is 115 GPa while that of the cortical bone is 10 to 26 GPa.

Nowadays, research on many metallic biomedical implants is done by focusing on β Ti alloys prepared with nontoxic elements because of their appropriated mechanical properties, such as low elasticity modulus, electrochemical stability, and high corrosion resistance in body-simulated media.[1–5]

Recently, Oliveira and colleagues[1] and Oliveira and Guastaldi[3,5] have studied Ti–Mo alloys to be applied as biomaterials. The X-ray diffraction (XRD) analysis showed that the crystal structure of Ti–Mo alloys is sensitive to the Mo concentration; the α" phase is observed almost exclusively when the concentration of Mo added to the Ti reaches 6%. A significant retention of the β phase is observed for the alloy containing 10% Mo, while at higher Mo concentrations (15 and 20%), retention of phase β is only verified.[1] They also found a Young's modulus of 80 GPa for a Ti–15Mo alloy (unpublished data). Electrochemical behavior of pure Ti and Ti–Mo alloys was investigated as a function of immersion time in electrolyte simulating physiological media.[3,5] All these electrochemical results suggest that the Ti–Mo alloys are promising to be applied in orthopedic devices, particularly in the case of Ti–15Mo since electrochemical stability is directly associated with biocompatibility and is a necessary condition for applying a material as biomaterial.[3,5]

Furthermore, another important aspect to be investigated is the morphology and physical–chemical properties of the implant surface, which is very important to osseointegration, to the healing time, to tissue regeneration, and finally, to implant working behavior.[11] Different techniques have been used in an attempt to either tailor or modify the implant surface such as mechanical methods, ion implantation, chemical treatment, sol-gel, plasma spray, and laser cladding.[6,12,13] Several authors have demonstrated higher percentage of bone-to-implant contact (BIC) as well as removal torque values for rough dental implant surface when compared with machined implants, showing a faster development of bone-implant integration.[13–15] In this regard, sandblasting, plasma spraying, and acid etching have become the three most common approaches used to alter the surface topography and increase the specific surface area of implants. But the main problem of those treatments is the contamination of the surface during the modification procedure.[16,17] On the other hand, Laser beam irradiation is a clean and reproducible process, where the implant surface does not interact with any other materials for its modification during the irradiation. Differently of others surface modification processes, with laser beam irradiation, it is possible to obtain different surfaces composition (e.g., Ti oxides and nitrides) by changing the applied fluency.[18] Therefore, with this irradiation process, it is possible to improve the implant surface characteristics, which may help the osseointegration phenomenon, such as morphology, surface area, roughness and different chemical composition, which change the physical–chemical properties of the surface and consequently their wettability.

Considering the potential of the laser ablation to create a stable surface on Ti and its alloys, the aim of the present study was to assess the in vivo bone response by removal torque, hystological and histometrical analysis on a recently developed biomedical Ti–15Mo alloy, installed in the tibia of rabbits after surface modification by laser beam irradiation.

MATERIALS AND METHODS

Alloy Preparation

The Ti–15Mo wt% alloy was casting in an arc-melting furnace under an ultrapure argon atmosphere, following a well-known procedure described in the literature.[1,19] Prior to implant preparation, Energy Dispersive X-ray Fluorescence (EDXRF) and Energy Dispersive X-ray (EDX) spectra were used to confirm that the ingots composition was close to nominal (15Mo wt%). The samples were cleaned in an ultrasonic bath with deionized water for 10 minutes, then with pure acetone for 10 minutes, and finally, with isopropilic alcohol for further 10 minutes. The chemical analyses were performed in a total of six different areas on the bulk and on the surface of each ingot by both techniques (EDXRF and EDX).

After chemical characterization, metallographic observation with Scanning Electron Microscopy (SEM) and mapping of Mo were performed on the samples' surface in order to verify possible defects from casting process and the distribution of Mo.

The experiments were conducted using a SEM microscope (LEO 440, LEO Electron Microscopy Ltd., Cambridge, UK) coupled with an energy dispersive analyzer [model 760 Si(Li)] with a resolution of 133 eV, while for EDXRF measurements, a fluorescence X-ray spectrometer (EDX-800 RayNy, Shimadzu, Kyoto, Japan) was used.

Laser Surface Modification

Previous and after the surface preparation, all samples were cleaned in an ultrasonic bath with deionized water for 10 minutes, then with pure acetone for 10 minutes, and finally, with isopropilic alcohol for further 10 minutes. This cleaning process was used in order to remove eventual organic and inorganic debris resulting from the implants and surfaces preparation process.

The surfaces of the samples used in this work were prepared with two different procedures: machined (MS) and modified by laser beam-irradiation (LS). The LS surfaces were obtained using a pulsed Yb laser (DML-100, Violin System Omnimark – Laser, Yb-pulsed, 20 W; OmniTek Tecnologia Ltda, São Paulo, SP, Brazil) working on air.

In order to perform the surface modification of the implants, the LS samples were fixed in a special device with its rotation controlled by computer. The surface with threads were positioned perpendicularly to the laser beam (Figure 1), and using the omnimark 2.0 software with a personal configuration, the laser was irradiated longitudinally on the surface followed by an automatic rotation of the implant after every laser scan. The sample rotation rate was adjusted in order to perform just one laser scan in every region of the surface.

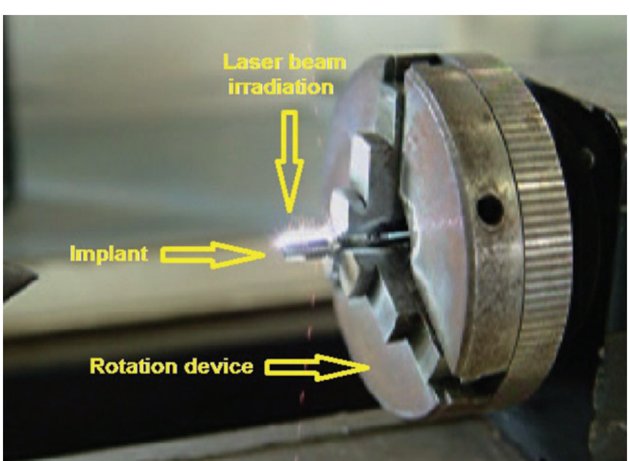

Figure 1 Laser beam irradiation setup.

Disks Preparation and Wettability Analysis

Disks (Ø 10 mm x 2 mm thickness) with MS and LS surfaces were prepared for contact angle measurements (OCA-15 video-based optical contact angle meter, Dataphysics Instruments GmBh, Filderstadt, German).

Previous and after surface preparation, all the samples were ultrasonically cleaned using the same procedure described in the item earlier. To reduce the effect of environmental moisture on the disks, especially on laser-treated samples, all contact angle measurements were made within 1 hour after treatment. For this measure, a minimum of three drops (demineralized water) were collected at different areas on the samples surface. All analyses were performed at room temperature.

Implants Preparation

After the characterization of chemical composition, the obtained ingots were cut and wide cylindrical dental implants were obtained (10 mm long and 3.75 mm in outer diameter) by a commercial company using a conventional lathe. One sample for each surface underwent presurgery SEM/EDX analysis in order to check the surface composition and topography prior to surgery. A total of 32 implants were divided into two groups: 16 MS implants (control samples) and 16 LS implants (Test samples). Six implants of each surface were used for removal torque test and 10 of each surface for histological and histometrical analysis.

After the implants preparation and their surface modification, the samples were cleaned using the procedure described earlier in the laser surface modification item, and then they were sterilized by gamma irradiation, using 25 kGy as a sterilizing dose, by a commercial company.

Surgical Procedure

Following approval of bioethics committee for animal experimentation of the Universidade Estadual Paulista (UNESP) (protocol 2008/003997), white New Zealand rabbits, 10 months old (weight 3–3.5 kg), were used in the present study. The surgery was performed at the Faculdade de Odontologia de Araçatuba, UNESP.

The animals were anesthetized with a combination of ketamine (0.35 mg/kg) and xylazine (0.5 mg/kg). Tibial metaphyses were then exposed by an incision in the proximal–distal direction of approximately 3 cm in order to place two implants into each tibiae. Each rabbit received four implants, two control ones in the left tibia and two laser in the right tibia. The preparation of the bone site was performed with burs under abundant irrigation with saline solution. The implant insertion procedure obeyed a progressive milling sequence, with the motor speed reduced to 20 rpm. After the implants insertion, the cover screws were placed and the soft tissues were sutured in layers; a single dose of antibiotic was given (0.25 g Cefazolin, IM) in the postoperative management. After an 8-week healing period, the animals were euthanized with an overdose of anesthetic.

Removal Torque Test

After implant exposure, a specially designed key was connected to the implant and the manual torque gauge manometer (15-BTG, Tohnichi, Japan-fundo de escala 100 Ncm; Tohnichi Mfg. Co. Ltd. of Tokyo, Japan). An anticlockwise movement was performed to remove the implant. The maximal torque value for breakage of bone-implant interaction was measured in Ncm. No forces were applied in the vertical direction to avoid alterations in the data.

Histological Analysis

After euthanasia of the animals, the implants were retrieved with a 4.0 mm-wide trephine.

The implants and the surrounding tissues were stored immediately in 10% buffered formalin and processed to obtain thin ground sections with the Precise 1 Automated System (Assing, Rome, Italy). The specimens were dehydrated in an ascending series of alcohol rinses and embedded in a glycolmethacrylate resin (Technovit® 7200 VLC, Kulzer, Wehrheim, Germany). After polymerization, the specimens were sectioned longitudinally along the major axis of the implant with a high-precision diamond disc at about 150 µm and ground down to about 30 µm. Three slides were obtained. The slides were stained with basic fuchsin and toluidine blue.

Histomorphometry of BIC percentage, defined as the amount of mineralized bone in direct contact with the implant surface, was measured as well as the BIC of the three best consecutive threads of each implant in the cortical bone region and also in marrow spaces. The measurements were carried out using a light microscope (Laborlux S, Leitz, Wetzlar, Germany) connected to a high-resolution video camera (3CCD, JVC KY-F55B, JVC, Yokohama, Japan) and interfaced to a monitor and a microcomputer (Intel Pentium III 1200 MMX, Intel, Santa Clara, CA, USA). This optical system was associated with a digitizing pad (Matrix Vision GmbH, Oppenweiler, Germany) and a histometry software package with image-capturing capabilities (Image-Pro Plus 4.5, Media Cybernetics Inc., Immagini & Computer Snc, Milano, Italy).

Statistical Analysis

Data from the histomorphometrical evaluations were analyzed using the nonparametric paired Mann-Whitney test. Results were presented as means ± standard deviation (SD), and differences at level of significance p when ≤.05 were considered statistically significant.

RESULTS

Chemical Analyses

The chemical analyses (EDXRF and EDX) showed that the actual chemical composition of the Ti–15Mo alloy was close to the nominal value in all cases (Table 1). The chemical composition of the alloy was homogeneous, and no expressive differences were found between surface and bulk with both techniques used ($p > .10$).

SEM analysis revealed surfaces without defects from the casting process (Figure 2A), while the mapping of Mo and Ti showed a homogeneous distribution of these elements, without preferential zone, in the whole analyzed region (Figure 2, B and C). The studies confirmed the efficiency of the method used, leading to obtain a homogeneous alloy, with the composition close to the nominal.

TABLE 1 EDX and EDXRF Analysis for Ti–15Mo Alloy Ingots Wt%

	Surface Mean ± SD	Bulk Mean ± SD	*p* Value*
EDX	15.13 ± 0.25	15.11 ± 0.26	>.9999
EDXRF	14.86 ± 0.19	15.14 ± 0.32	.2499

*The two-tailed p values .2499 and >.9999 are considered not significant.

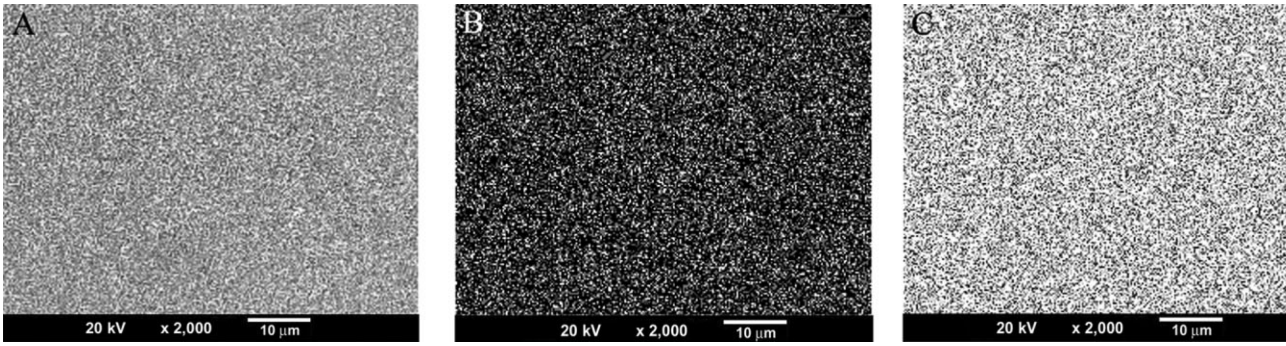

Figure 2 (A) SEM micrograph of Ti–15Mo alloy sample; (B) Mo mapping (white points); (C) Ti mapping (*white points*) on the same surface. Magnification ×2,000.

Presurgery Implant Surface Characterization

In order to characterize the surface morphology modifications before the surgical procedure, EDXRF and SEM/EDX analyses were performed. It was possible to observe differences in the surface topography between machined and laser-treated implants. The control samples (MS) showed a smooth surface (Figure 3, A–C), while the test ones (LS) presented irregular-shaped cavities on its surface and a typical macrostructured/microstructured surface with large depressions (Figure 4, A–C). The oxygen peak was totally absent in the control group (Figure 3D) and was only found in the test group (Figure 4D) by EDX analyses. This was due to the fact that laser surface was produced by Ti fusion in the air (i.e., in the presence of O_2). No other extraneous elements apart from these alloy constituents were identified, confirming lack of chemical contamination of the surface.

Wettability Analysis

Contact angle measurements (0° ≤ contact angle ≤ 90°) were carried out in order to evaluate the wettability of the surface-modified alloy as resulting from laser beam treatment. Demineralized water put on MS samples formed a regular drop, with a contact angle of 77.97 ± 5.06°, while the water spreads completely on the

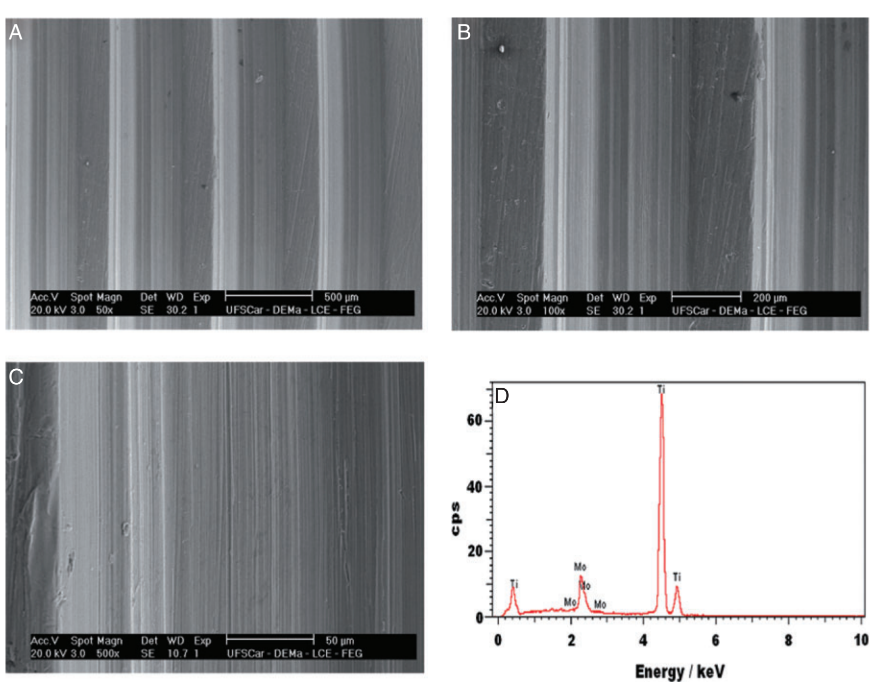

Figure 3 SEM micrographies showing the morphology of Ti–15Mo alloy implants with machined surface (MS) – control group: (A) ×50; (B) ×100; (C) ×500; (D) EDX of the same surface.

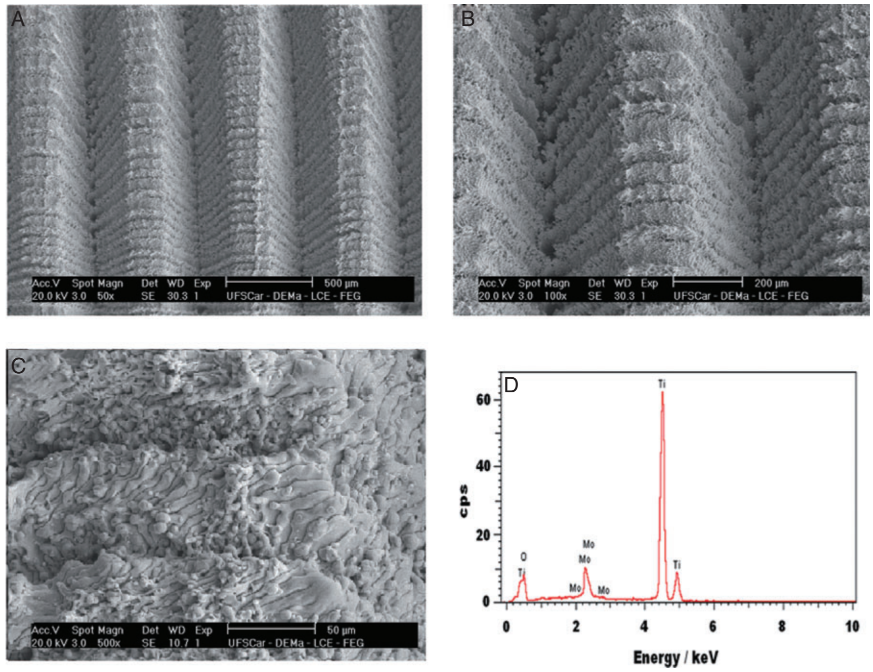

Figure 4 SEM micrographies showing the topography of Ti–15Mo alloy implants with laser beam-irradiated surface (LS) – test group: (A) ×50; (B) ×100; (C) ×500; (D) EDX of the same surface.

surface of LS samples (contact angle 0°), showing that laser surface treatment presents a great influence on the wettability of Ti–15Mo surface.

Clinical Observations

Animal surgical procedures and follow-up demonstrated no complications regarding procedural conditions, postoperative infection, or other clinical concerns. During the healing period, one rabbit died, and thus, two machined and two laser implants were lost.

Removal Torque Measurements

In general, the animals presented no disturbances in soft tissue healing or tibia fractures. There was no detection of any alteration on the surfaces during the implant insertion or removal processes. The mean and SD of removal torque by group in the period of evaluation are summarized in Table 2.

Since the limit of the torque wrench used in the study is 90 Ncm, all LS implants were not removed by the biomechanical test, and consequently will be just presented the mean and standard deviation of the MS implants.

Histological Results

MS Implants (Control Samples). Histological evaluation showed the presence of bone tissue originating predominantly from preexistent cortical bone for machined implants (Figure 5A). The coronal portion of the implant and the upper threads were not in contact with the bone tissue because the implants did not completely fit the artificial alveoli as they were longer than the rabbit tibiae diameter.

TABLE 2 Mean and Standard Deviation of Removal Torque Machined (MS) and Laser-Treated (LS) Implants in the Period

		Torque (Ncm)	
	Rabbits	MS	LS*
	1	55	>90
	2	32	>90
	3	38	>90
	4	63	>90
	5	55	>90
	6	66	>90
Average		51.5	—
Standard Deviation		13.63	—

*Above the detection limit of the manual torque gauge manometer.

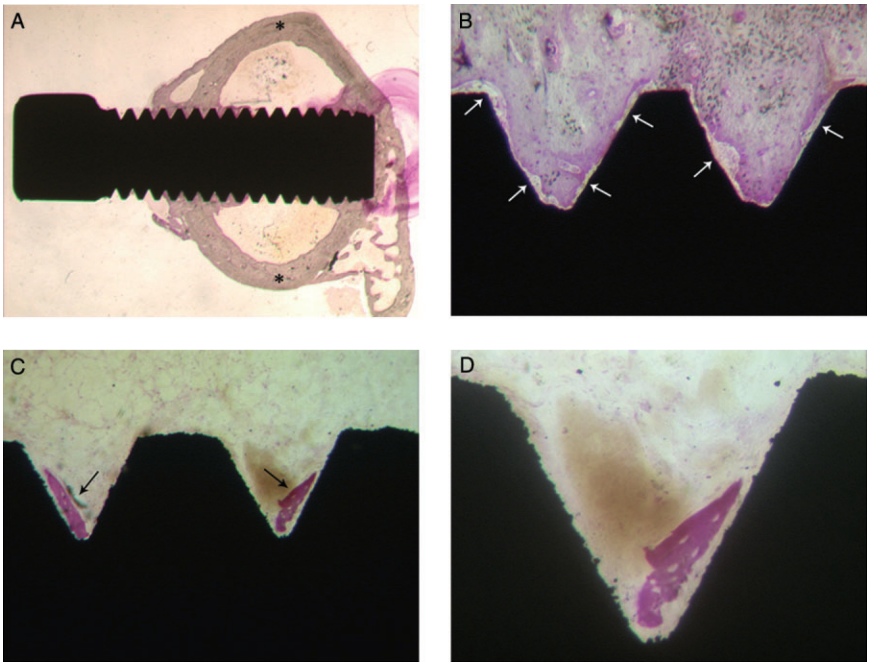

Figure 5 Light microscopic pictures of Ti–15Mo alloy implant with machine-surfaced – MS (control group) – acid fuchsin-toluidine blue: (A) image showing the whole implant surrounded by bone tissue originating predominantly from preexistent cortical bone (*asterisks*) – ×8;(B) in the cortical region, it was possible to observe compact bone tissue with small marrow spaces, and in most of the surface, a gap (*arrows*) could be detected at the interface – ×40; (C) in the marrow spaces of the best three consecutive threads, small newly formed trabeculae (*arrows*) were predominantly located in the thread concavities – ×40; (D) at high power, in the medullary region, a gap between the bone and the newly formed trabecula was present – ×200.

In the cortical region along implant perimeter, compact bone tissue with small marrow spaces could be observed in the MS implants. However, a direct contact between bone and implant surface was present only in very few areas for the MS samples; in most of the surface, a gap could be observed at the interface (Figure 5B).

In the marrow region, small newly formed trabeculae within the implant threads of the machined implants could be observed; these were not homogeneously distributed, and at higher magnification, it was possible to observe that they were predominantly located in the thread concavities with a gap at the bone-implant interface and the presence of a thin layer of connective tissue (Figure 5C). In the marrow region, a gap between the bone and the newly formed trabeculae was present (Figure 5D).

LS Implants (Test Samples). Histological evaluation showed the presence of bone tissue originating predominantly from preexistent cortical bone for the LS implants. In the cortical region along the implant perimeter, compact bone tissue with small marrow spaces could be observed in the laser-treated implants (Figure 6A). Moreover, in the LS implants, the bone tissue perfectly filled the surface irregularities, without a gap at the bone-implant interface (Figure 6B).

In the marrow region, a thin layer of newly formed bone tissue could be found in close contact with the LS surface (Figure 6C), homogeneously distributed all along the implant perimeter, either in the concavity or in the convexity of the threads. Large osteocyte lacunae typical of newly formed bone could also be observed at direct contact with the surface (Figure 6D).

Histomorphomometry

Histomorphometric data showed a significant statistical difference between the control and the test groups regarding BIC %: 24.07% and 41.88%, respectively ($p = .0012$). Moreover, a significant statistical difference between the MS and LS implants was also found evaluating the three best consecutive treads of the cortical ($p = .0012$) and marrow ($p = .0082$) regions (Table 3), confirming the great influence of the laser beam treatment on the histologic and histomorphometric response of the Ti–15Mo alloy.

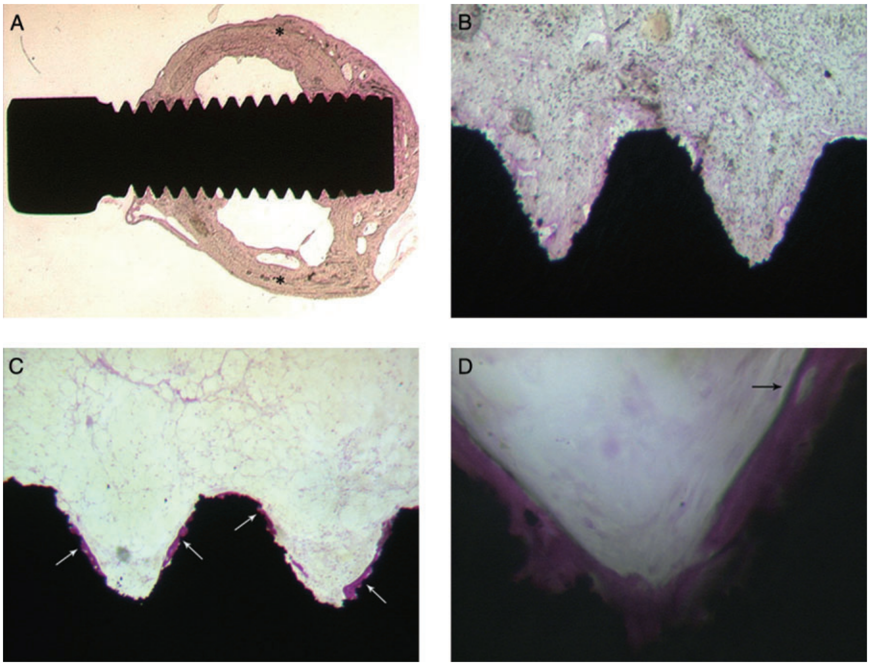

Figure 6 Light microscopic pictures of Ti–15Mo alloy implant with laser beam-irradiated surface – LS (test group) – acid fuchsin-toluidine blue: (A) image showing the presence of compact bone tissue with small marrow spaces originating predominantly from preexistent cortical bone (*asterisks*) – ×8; (B) in the cortical bone region, the bone tissue perfectly filled the surface irregularities, without a gap at the bone-implant interface – ×40; (C) in the medullary region of the best three consecutive threads, a thin layer of newly formed bone tissue (*arrows*) could be found in close contact with the implant surface – ×40; (D) at high power, bone tissue homogeneously distributed all along the implant perimeter; large osteocyte lacunae (*arrow*) typical of newly formed bone, could also be observed at direct contact with the surface – ×200.

DISCUSSION

In the past years, several modifications of specific surface properties such as topography, structure, chemistry, surface charge, and wettability have been investigated to predictably improve the osseointegration of Ti implants.[20] Close attention has been paid to a higher surface energy and increased wettability since both properties have been shown to enhance the interactions between a surface and its biologic environment.[20] The terms wetting as employed in various practical situation tend to be defined in terms of the effect desired. Usually, however, wetting means that the contact angle between a liquid and a solid is zero or so close to zero that the liquid spreads over the solid easily.[21] The initial interaction between living bone and tissue and implant surface occurs as the surface of the implant biomaterial is exposed to tissue fluids. This produces a layer of macromolecules and fluids, which influences the behavior of cells when they encounter the implant surface. Following these events, a series of cell material interactions takes place, leading to the release of growth

TABLE 3 Mean and Standard Deviation of Bone-to-Implant Contact Percentages (BIC%) for the Best Three Consecutive Threads of Cortical Bone Region and Marrow Spaces of Machined (MS) and Laser-Treated (LS) Implants

	MS Mean ± Standard Error	LS Mean ± Standard Error	*p* Value*
	24.07 ± 3.26	41.88 ± 3.20	.0012
Cortical bone	41.54 ± 2.43	85.87 ± 3.08	.0012
Medullary spaces	11.18 ± 0.93	31.83 ± 4.92	.0082

*The two-tailed *p* values .0012 and .0082 are considered very significant.

and chemotactic factors that may modulate cellular activity in the surrounding tissue.[22] Then, wettability may be one of the surface factors to be considered when selecting dental and orthopedic implant biomaterials. The ability of a liquid to wet the surface of a solid is influenced by a number of factors such as the roughness of the surface, the cleanliness of the surface, and the surface energy.[22]

In the present work, contact angle measurements were carried out in order to evaluate the wettability of the surface-modified alloy as resulting from laser treatment. Laser surface treatment showed a great influence on the wettability of Ti–15Mo surface. The null contact angle measured for test disks indicated that the laser treatment used in this work is effective to improve hydrophilicity on the Ti–15Mo alloy surface. According to Mekayarajjananonth and Winkler[22] and Spriano and colleagues,[23] low contact angles (below 30°) indicate good wetting (the liquid must spreads easily over the entire surface and adhere to the solid surface[21]) and are promising for a successful osteointegration.

On the other hand, several authors have demonstrated higher percentage of BIC as well as removal torque values for modified implant surfaces when compared with machined ones.[13–15,17,24–28]

The resistance of implants to removal torque has been used in several animal studies to evaluate osseointegration and it is related to the integration grade between the mineralized bone and the surface structures.[29–33] This resistance can be correlated to the degree of physicochemical interaction between mineralized bone and the implant surface.[33,34] Thus, the implant removal torque is influenced by the adjacent mechanical bone properties, in quality and quantity, and the degree of bone-implant contact.[33,35] Under healthy conditions, bone remodeling occurs progressively, increasing the degree of BIC and consequently increasing the torque needed to remove the implant.[31,36]

In the present study, laser surface treatment showed a great influence on the removal torque test and histological and histomorphometrical response of the Ti–15Mo alloy. The results suggest that the LS implants had an acceleration at the anchorage process. This fact can be related to the physical–chemical properties and to the increase at the implant/bone tissue contact area, which is caused by the surface modification. It was possible by SEM to observe that the surface modified by laser beam resulted in a complex surface morphology, increasing the specific area and bone-implant contact interface.

The removal values of reverse torque obtained in this study are concordant with the histological and histomorphometrical results, which showed a significantly higher BIC % for laser implants both in the cortical and medullary regions, with the bone tissue perfectly filling the surface irregularities without gaps at the bone-implant interface. All these results are showing that the physical–chemical properties created by laser irradiation on the LS samples induct a better interaction between the implant surface and the neo-formed bone, leading to higher removal torque values.

These data are supported by other studies presented in the literature where implant surface topography was modified by laser beam irradiation.[24–28] Using Nd:YAG laser, Hallgren and colleagues[27] found 40% of bone-implant contact for implants modified by laser and 32% for machined implants. The reverse torque removal experiment showed a mean value of 52 Ncm for implants treated by laser and 35 Ncm for machined implants after 12 weeks of healing. A similar behavior was found by Cho and Jung,[25] comparing the reverse torque removal values of implants with machined surfaces and surfaces modified by laser after 8 weeks of implantation. The value of reverse torque removal was 23.58 ± 3.71 Ncm for machined implants and 62.57 ± 10.44 Ncm for implants modified by laser. In another work, Karacs and colleagues[28] compared the removal by reverse torque of implants with machined surfaces, sand-blasted surfaces and sand-blasted surfaces in association with laser beam irradiation. The authors observed that the laser treatment after sand-blasting increased almost 50% the removal by reverse torque.

CONCLUSIONS

Within the limitations of the present study, the results demonstrated that all implants were osseointegrated after 8 weeks and the process of surface modification of implants with laser irradiation besides being a clean process, reproducible, and with low cost improved the properties of osseointegration of the Ti–15Mo alloy. The laser modification produces a surface with important and appropriated properties for osseointegration, increasing bone-implant retention, and resulting in a better and faster integration of them.

The biomechanical data suggested that the implants with laser surface modification can shorten the implant healing period by the increase of bone-implant interaction and also showed a great influence on the wettability and BIC % of Ti–15Mo surface, achieving statistically significant higher values when compared with the machined control group.

Therefore, this surface modification allowed to obtain surface with important physical–chemical and morphological properties and characteristics appropriated to be used as dental and orthopedics implants, showing that laser-treated Ti–15Mo alloys are promising materials for implants application.

ACKNOWLEDGMENTS

The authors are grateful to FAPESP for scholarships (proc. 04/11751–8, 08/04867–0 and 08/02073–7) and grants (Proc. 05/04050–6) that made this work possible. They also thanks Prof. Dr. Carlos R. Grandini and his co-workers, Grupo de Relaxações Anelásticas of the Faculdade de Ciências de Bauru – Departamento de Física – UNESP – Bauru for their help for the casting of the alloys, Dr. Thallita P. Queiroz for helping with the animals surgery, and Dr. Hewerson Tavares and MSc Rafael Bini for helping with laser treatments.

This work was partially supported by the National Research Council, Rome, Italy, by the Ministry of Education, University and Research, Rome, Italy.

REFERENCES

1. Oliveira NTC, Aleixo G, Caram R, Guastaldi AC. Development of Ti–Mo alloys for biomedical applications: microstructure and electrochemical characterization. Mat Sci Eng A – Struct Mater 2007; 452–453:727–731.
2. Kuroda D, Niinomi M, Morinaga M, Kato Y, Yashiro T. Design and mechanical properties of new β type titanium alloys for implant materials. Mat Sci Eng A 1998; 243:244–249.
3. Oliveira NTC, Guastaldi AC. Electrochemical behavior of Ti–Mo alloys applied as biomaterial. Corrosion Sci 2008; 50:938–945.
4. López MF, Gutiérrez A, Jiménez JA. In vitro corrosion behaviour of titanium alloys without vanadium. Electrochim Acta 2002; 47:1359–1364.
5. Oliveira NTC, Guastaldi AC. Electrochemical stability and corrosion resistance of Ti–Mo alloys for biomedical applications. Acta Biomater 2009; 5:399–405.
6. Singh R, Chowdhury SG, Tiwari SK, Dahotre NB. Laser surface processing of Ti6Al4V in gaseous nitrogen: corrosion performance in physiological solution. J Mater Sci Mater Med 2008; 19:1363–1369.
7. Morant C, López MF, Gutiérrez A, Jiménez JA. AFM and SEM characterization of non-toxic vanadium-free Ti alloys used as biomaterials. Appl Surf Sci 2003; 220:79–87.
8. Rivera-Denizard O, Diffoot-Carlo N, Navas V, Sundaram PA. Biocompatibility studies of human fetal osteoblast cells cultured on gamma titanium aluminide. J Mater Sci Mater Med 2008; 19:153–158.
9. Okazaki Y, Rao S, Tateishi T, Ito Y. Cytocompatibility of various metal and development of new titanium alloys for medical implants. Mat Sci Eng A 1998; 243:250–256.
10. Ku CH, Pioletti DP, Browne M, Gregson PJ. Effect of different Ti–6Al–4V surface treatments on osteoblasts behaviour. Biomaterials 2002; 23:1447–1454.
11. Bathomarco RV, Solorzano G, Elias CN, Prioli R. Atomic force microscopy analysis of different surface treatments of Ti dental implant surfaces. Appl Surf Sci 2004; 233:29–34.
12. Das K, Balla VK, Bandyopadhyay A, Bose S. Surface modification of laser-processed porous titanium for load-bearing implants. Scr Mater 2008; 59:822–825.
13. Grassi S, Piattelli A, Ferrari DS, et al. Histologic evaluation of human bone integration on machined and sandblasted acid-etched titanium surfaces in type IV bone. J Oral Implantol 2007; 33:8–12.
14. Grassi S, Piattelli A, de Figueiredo LC, et al. Histologic evaluation of early human bone response to different implant surfaces. J Periodontol 2006; 77:1736–1743.
15. Shibli JA, Grassi S, de Figueiredo LC, et al. Influence of implant surface topography on early osseointegration: a histological study in human jaws. J Biomed Mater Res B Appl Biomater 2007; 80:377–385.
16. Gaggl A, Schultes G, Muller WD, Karcher H. Scanning electron microscopical analysis of laser-treated titanium implant surfaces – a comparative study. Biomaterials 2000; 21:1067–1073.
17. Marticorena M, Corti G, Olmedo D, Guglielmotti MB, Duhalde S. Laser surface modification of Ti implants to improve osseointegration. J Phys Conf Ser 2007; 59:662–665.
18. Braga FJC, Marques RFC, Filho EA, Guastaldi AC. Surface modification of Ti dental implants by Nd:YVO4 laser irradiation. Appl Surf Sci 2007; 253:9203–9208.
19. Oliveira NTC, Biaggio SR, Piazza S, Sunseri C, Di Quarto F. Photo-electrochemical and impedance investigation of passive layers grown anodically on titanium alloys. Electrochim Acta 2004; 49:4563–4576.
20. Schwarz F, Wieland M, Schwartz Z, et al. Review potential of chemically modified hydrophilic surface characteristics to support tissue integration of titanium dental implants. J Biomed Mater Res B Appl Biomater 2009; 88B:544–557.
21. Adamsom JW, Gast AP. The solid-liquid interface – contact angle. In: Physical Chemistry of Surfaces. New York: John Wiley & Sons, Inc., 1997:465–468.

22. Mekayarajjananonth T, Winkler S. Contact angle measurement on dental implant biomaterials. J Oral Implantol 1999; 25:230–236.
23. Spriano S, Bosetti M, Bronzoni M, et al. Surface properties and cell response of low metal ion release Ti–6Al–7Nb alloy after multi-step chemical and thermal treatments. Biomaterials 2005; 26:1219–1229.
24. Gotz HE, Muller M, Emmel A, Holzwarth U, Erben RG, Stangl R. Effect of surface finish on the osseointegration of laser-treated titanium alloy implants. Biomaterials 2004; 25:4057–4064.
25. Cho SA, Jung SK. A removal torque of the laser-treated titanium implants in rabbit tibia. Biomaterials 2003; 24:4859–4863.
26. Wennerberg A, Albrektsson T, Johansson C, Andersson B. Experimental study of turned and grit-blasted screw-shaped implants with special emphasis on effects of blasting material and surface topography. Biomaterials 1996; 17:15–22.
27. Hallgren C, Reimers H, Chakarov D, Gold J, Wennerberg A. An in vivo study of bone response to implants topographically modified by laser micromachining. Biomaterials 2003; 24:701–710.
28. Karacs A, Joob Fancsaly A, Divinyi T, Peto G, Kovach G. Morphological and animal study of titanium dental implant surface induced by blasting and high intensity pulsed Nd-glass laser. Mater Sci Eng C 2003; 23:431–435.
29. Gotfredsen K, Berglundh T, Lindhe J. Bone reactions adjacent to titanium implants with different surface characteristics subjected to static load. A study in the dog (II). Clin Oral Implants Res 2001; 3:196–201.
30. Buser D, Mericske-Stern R, Bernard JP, et al. Long-term evaluation of non-submerged ITI implants. Part I. 8-year life table analysis of a prospective multi-center study with 2359 implants. Clin Oral Implants Res 1997; 8:161–172.
31. Johansson C, Albrektsson T. Integration of screw implants in the rabbit. A 1-year follow-up of removal torque of titanium implants. Int J Oral Maxillofac Implants 1987; 2:69–75.
32. Margonar R, Sakakura CE, Holzhausen M, Pepato MT, Alba RC, Marcantonio E Jr. The influence of diabetes mellitus and insulin therapy on biomechanical retention around dental implants: a study in rabbits. Implant Dent 2003; 12:333–339.
33. Sennerby L, Thomsen P, Ericson LE. A morphometric and biomechanic comparison of titanium implants inserted in rabbit cortical and cancellous bone. Int J Oral Maxillofac Implants 1992; 7:62–71.
34. Carlsson L, Rostlund T, Albrektsson B, Albrektsson T. Removal torques for polished and rough titanium implants. Int J Oral Maxillofac Implants 1988; 3:21–24.
35. Ivanoff CJ, Widmark G, Johansson C, Wennerberg A. Histological evaluation of bone response to oxidized and turned titanium microimplants in human jawbone. Int J Oral Maxillofac Implants 2003; 18:341–348.
36. Sakakura CE, Margonar R, Holzhausen M, Nociti FH Jr, Alba RC, Marcantonio E Jr. Influence of cyclosporin-a therapy on bone healing around titanium implants. A histometric and biomechanic study in rabbits. J Periodontol 2003; 74:976–981.